

Matthew Gardiner

Metrics for Evaluating Origami Regularity

1.1 Abstract

In the era of Computational Origami, a new class of folding pattern has arisen, the irregular pattern. In this study, I examine the proposition that the regularity of a crease pattern is an additional factor in evaluating what determining *difficulty-based-foldability*, or *how complex is the task of folding a given crease pattern?*. To understand this problem beyond subjective origami difficulty as signments, a set of metrics are introduced to analyse the geometric properties of crease patterns, including: parallelity, edge length equality, angle equality, angle regularity, fold density and angle divisibility; to calculate a difficulty-based-foldability value known as the *Origami Regularity Index* (using the abbreviation: *R.I.*). Patterns with high R.I. values, between 0.75-1.0, are considered regular and easier to fold, low R.I. values are considered irregular and therefore become more difficult to fold. This index is evaluated as a float between 0.000 and 1.000, with 1.000 being perfect foldability and 0.000 being the hardest possible ranking of Origami Regularity, and therefore, the most difficult foldability.

1.2 Rationale

The term foldability can be understood to mean the ability of the material to be folded, including the force required to bend the material, and the pliability of the

material to accept the fold. General foldability in origami is subjective¹ within the origami community, difficulty is often assigned by the author or publisher, using such terms as: beginner, intermediate, advanced and super complex (OrigamiUSA, n.d.). This study doesn't seek to supercede these difficulty rankings, but rather to determine and evaluate the geometric properties of origami patterns, and to design a process by which these properties can be examined and compared to one another.

Origami patterns designed that are designed *by-hand* are *by-and-large* regular designs. One reason is that the folding lines are determined by geometric ratios found within the paper, such as divisions of the square angles of the sheet, wherein two main angle sets emerge: dividing in half (resulting in 90/45/22.5 patterns) or dividing in thirds (resulting in 90/60/30/15). Other approaches such as regular divisions of the sheet into a grid such as the box-pleating method have design complexity with high-regularity. The area of computational origami can quickly produce irregular divisions of angles. Robert Lang in his introduction of ReferenceFinder (Lang, Robert, 2007) discusses a this difficulty introduced by compuational origami:

“This didn’t used to be a problem. In the traditional “trial-and-error” approach to origami composition, the design was discovered via exploration of folding“.

With Lang’s design program TreeMaker a design can require eccentric and non-paper defined locations, divisions and angle sets. A more complex problem is that posed by crease patterns generated in software such as FreeForm Origami (T Tachi, 2010). The patterns can have little or no parallelity or angle symmetry, giving the folder no way to use the material to generate the sequence of folds. Such patterns require digital fabrication or advanced production techniques to transfer the pattern to the paper. Digital fabrication solves the problem of finding and marking the creases, but in many cases does not solve the problem of actually folding it. A digitally fabricated pattern with high regularity will still be easier to fold than a digitally fabricate irregular pattern, as a regular pattern still offers geometric utility in crease forming and fold actuation.

¹OrigamiUSA’s guidelines for difficulty are designed to address issues of teaching at the yearly conventions. The criteria are very reasonable and for their purposes complete, and consider the difficulty of particular origami choreographies such as types of folds, i.e. closed sinks, open sinks, and folding from crease patterns where landmarks may be obscure and need to be determined by the folder on-the-fly.

This study is preliminary, based on the proposition that *regular* origami patterns are easier to fold than *irregular* patterns, and therefore, regularity is a useful metric in determining the difficulty in folding an origami pattern. It is a known problem that some origami is harder than others, but how hard is it to fold something complex? The metrics outlined in this study are the beginning of an analytical tool towards evaluating how complex an origami crease pattern is to fold.

1.3 Related Work

Specific cases of foldability have existing analytical methods such as flat-foldability evaluation by Maekawa and Kawasaki's theorems (Kawasaki, 1989, Kasahara and Takahama (1998), Hull (1994)), and rigid-foldability for evaluating kinetic properties (Tachi, 2009, Tachi (2007), Demaine and Demaine (2002)). Material properties of folds in paperboard vs a perfect hinge are given as a measure of material-foldability in (Paperboard, 1993, pp. 186–193), and density of folds is factored in pattern optimisation by (Dudte et al., 2016). The class of pattern generated by software and algorithms (Demaine and Tachi, 2010), and (Tomohiro Tachi, 2010), are exceptionally complex to fold due to the irregularity of geometric properties in the pattern, as the algorithm, not a by-hand folding process, determines the location of the creases. The issue of difficulty to fold, is a combination of flat-foldability, material-foldability and other properties. The issue of regularity does not occur as a subject of study within literature, rather it is implied in the process of origami itself. Almost too obvious, it has been largely ignored, as most origami requires regularity to actually be foldable with repeatability. The concept of a *landmark* in origami, is a location that can be found by the process of folding edges, corners or other folds to one another. The aesthetic of irregularity is apparent in the works of Master Akira Yoshizawa's works, where the exact location of creases are not landmarked, and one can see in his works, the natural poses and expressions, are not repeated, rather they are nuanced and deliberate strokes by the artist.

This set of metrics, outlined in 1.4 are based on the assumption that a regular pattern is *easier* to fold than an irregular pattern and aims by geometric analysis, to create a new ranking for foldability based on regular-foldability. The metrics are designed to be extended as new metrics are discovered, as each new metric adjusts the overall index within the same value range. The statistical result is

evaluated as a ratio between 0 and 1, with 1 being perfectly regular, and easiest, and 0 being the most irregular, and hardest, ranking of the index.

1.4 Metrics of the Origami Regularity Index (R.I.)

This idea was inspired by a talk on Parametric Origami Design by Brian Chan at the Convention for Creators in Lyon in 2017, where his design process in Solid-works (normally a 3D CAD program) was being used for 2D CAD design of crease patterns. Chan was using the sketch constraints system to ensure that creases were parallel, equal lengths, in half, or at set origami angles, with the aim to make the pattern more foldable. This concept made me reflect on the completely irregular nature of the crease patterns generated in my parametric design process, and started my thinking on geometric regularity of creases in general.

This preliminary study aims to discover the geometric properties of regular and conversely, irregular patterns. A regular pattern has properties such as folds located on landmarks, parallel, perpendicular, or fold-based divisions such as $45/22.5^\circ$, or $15/30/60^\circ$, and on equally spaced grid: adjacent folds that have utility in forming the next fold. An irregular pattern has no landmarks, it is totally irregular, as adjacent folds have no utility in forming the next fold it therefore has low-foldability.

The following metrics are used to evaluate the regularity of a given crease pattern. The measurements are *parallelity*, *length equality*, *angle regularity*, *angle divisibility*, and *angle foldability*. These metrics collectively give a numerical value for fold complexity with regard to geometric regularity of a folding pattern. The metrics are evaluated through a point system. Each individual metric is a ratio value between zero and one. Each metric is worth one point. One being the maximum value representing perfect regularity of the metric, and zero being the least regular. The final value, the *Origami Regularity Index* is expressed as a ratio between zero and one. Calculated as an average, or sum of values divided by the number of values. The process for calculating each metric is the same, a script calculates the total number of property values, sums the equal values within tolerance, and calculates a ratio between the two.

The R.I. does not consider layered folds, or the complexity of choreographing certain multi-fold moves, but rather the properties of geometric arrangement of folds in relation to each other. Nor does it consider the material properties that

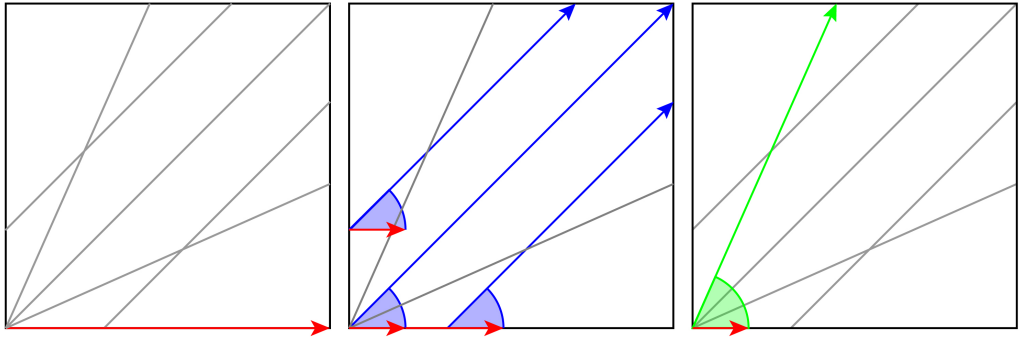


Figure 1.1: **Parallelity** From left: A sample crease pattern with baseline vector in red; parallel creases highlighted in blue, showing angle to red baseline vector; a green fold line with no parallelity.

determine material foldability, such as stiffness, elasticity and force required to break a fold. In this evaluation the edges of the paper are treated equivalently to a crease.

The following metrics were deduced from considering the impact of regularity in the formation of creases. Regularity in these metrics are evaluated as an overall average, the total of matching instances divided by the total number of instances in the pattern. This method is aimed at expedience, and can overall be considered an approximation. A more detailed analytic method could be developed to determine the actual utility of each individual crease, and resulting intersections in the formation of folding patterns, including the sequential steps required, however given the combinatorical nature of that kind of analysis, the algorithm will be computationally complex and require extended processing time. In contrast, the target method is to develop a tool to make a statistical estimate on the foldability of a pattern, and to execute and calculate quickly.

1.4.1 PARALLELITY

Let L be the total number of lines in the pattern

Let L_P be the number of lines parallel to at least one other line in the pattern

$$\text{Parallelity} = \frac{L_P}{L} \quad (1.1)$$

Parallelity is the measure of the number of lines that are parallel to at least one other line in the pattern. Parallel folds are easier to make as each parallel fold is a reference to another parallel fold. The principle is illustrated in Origami Axiom 3

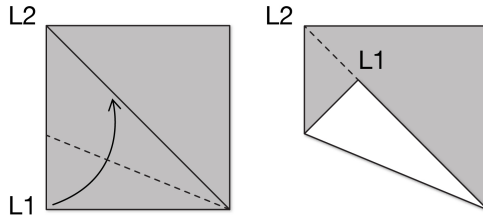


Figure 1.2: **Origami Axiom 3:** Given two lines, line 1 and line 2, there is a fold that places line 1 onto line 2.

(see Figure 1.2) where two lines are used to make a fold, n.b. the illustration does not show parallel lines, but the same principle can be applied any pair of lines, including parallel fold lines.

To measure parallelity in the set of crease patterns, a script evaluates a flattened mesh of the crease pattern by doing the following:

- Parallelity**
1. Calculate the angle of the fold with respect to a baseline (shown as a red vector in Figure 1.1, this difference is θ_g **global angle**. Calculated as the dot product between the baseline \mathbf{b} vector $(1,0,0)$ and \mathbf{f} the vector expression of the fold line . $\theta_g = \arccos \mathbf{b} \cdot \mathbf{f}$
 2. compare each fold to every other fold, if they have the same global angle, the fold lines are parallel.
 3. allow for a tolerance, the script evalutates up to 0.1° of tolerance.²
 4. sum all of the parallel folds, and divide by the total number of folds.

Therefore, perfect parallelity is where every fold is parallel to at least one other fold within a given tolerance. Parallelity is a ratio between zero and one. Where one is perfect parallelity and zero is complete non-parallelity.

1.4.2 LENGTH EQUALITY

Let L be the total number of lines in the pattern

Let L_E be the number of lines of length equal to at least one other line in the pattern

²Materials such as a fine washi paper *could* be expertly folded accurately down to $\pm 0.1^\circ$, or less, depending on the creasing method and dimensional accuracy of the sheet. A reasonable expectation for tolerance in a digital fabrication system such as a laser cutter or 3D printer driven by stepper motors is commonly $\pm 0.1\text{mm}$ to ± 0.01 positional accuracy at best. At most, this equates to an error range of $\pm 0.05^\circ$ over 100mm ($\arctan(0.1/100)$), or 0.1° range of tolerance.

$$LengthEquality = \frac{L_E}{L} \quad (1.2)$$

Equal length edges are common in patterns with high regularity, it is a quality that is found in symmetrical crease patterns, every fold line across the mirror line has at least one other fold line of the same length. It is also a quality that is found in regular tessellations of unit patterns, as the unit is repeated, so are the edge lengths. Equal edge lengths can indicate the possibility to use one edge to fold another.

To measure Length Equality in the set of crease patterns, a script evaluates a flattened mesh of the crease pattern by doing the following:

- Length Equality**
1. calculate the lengths of every given fold line (edge).
 2. sum all edges equal to at least one other edge within tolerance.
 3. divide the sum of edges with the total number of edges.

1.4.3 LENGTH EQUALITY INVERSE RATIO

Let L be the total number of lines in the pattern

Let L_U be the number of lines of unique length in the pattern

$$LengthEqualityInverseRatio = 1 - \frac{L_U}{L} \quad (1.3)$$

This measures and favors a crease pattern with a small number of unique edge lengths. The most simple form would be a straight pleat or grid that produces a folding pattern of only one edge length.

To measure Length Equality Inverse Ratio in the set of crease patterns, a script evaluates a flattened mesh of the crease pattern by doing the following:

- Length Equality Inverse Ratio**
1. calculate the lengths of every given fold line (edge).
 2. sum the unique edge lengths.
 3. divide the sum of unique edge lengths with the total number of edges and subtract from one.

1.4.4 ANGLE EQUALITY

Let A be the total number of angles in the pattern

Let A_E be the number of angles equal to at least one other angle in the pattern

$$\text{AngleEquality} = \frac{A_E}{A} \quad (1.4)$$

Perfect *Angle Equality* is where every fold angle, in relation to the vertex, is equal to at least one other angle length within a given tolerance. Angle Equality indicates a regularity in the pattern due to repetition of the same structure, as in tessellation, or in symmetrical patterns.

To measure Angle Equality in the set of crease patterns, a script evaluates a flattened mesh of the crease pattern by doing the following:

- Angle Equality**
1. calculate the angle of each fold line (edge) around each vertex.
 2. sum all angles with angle equality within tolerance.
 3. divide the sum of equal angles with the total number of angles.

1.4.5 UNIQUE ANGLE INVERSE RATIO

Let A be the total number of angles in the pattern

Let A_U be the number of unique angles in the pattern

$$\text{AngleEqualityInverseRatio} = 1 - \frac{A_U}{A} \quad (1.5)$$

In cases where the number of unique angles is high, the Origami Foldability is expected to be lower than a crease pattern with less unique folds. To measure the number of unique values. It is assumed that a high number of unique angles in an origami pattern is more irregular than a pattern with a fewer number of unique angles.

To measure Angle Equality Inverse Ratio in the set of crease patterns, a script evaluates a flattened mesh of the crease pattern by doing the following:

- Length Equality Inverse Ratio**
1. calculate the angle of each fold line (edge) around each vertex.
 2. sum the unique angles.
 3. divide the sum of unique angles with the total number of angles and subtract from one.

1.4.6 ANGLE REGULARITY

Let A be the total number of angles in the pattern.

Let A_R be the number of angles in the pattern that match 180° , 157.5° , 135° , 112.5° , 90° , 67.5° , 45° , 22.5° , 11.25° , 165° , 150° , 120° , 105° , 75° , 60° , 30° , 15° and 7.5° .

$$\text{AngleRegularity} = \frac{A_R}{A} \quad (1.6)$$

Angle Regularity is evaluated by examining the division of angles around a vertex for common origami angles that are c of 22.5° , and 15° , as they are equally divisible, thus making them easy to fold using adjacent folds derived from square origami sheets. Angle Regularity makes patterns more foldable as the folding angles are found with basic fold divisions 90° sheet corners.

To measure Angle Regularity in the set of crease patterns, a script evaluates a flattened mesh of the crease pattern by doing the following:

- Angle Regularity**
1. calculate the angle of each fold line (edge) around each vertex.
 2. sum the number of angles that are regular within tolerance to 180° , 157.5° , 135° , 112.5° , 90° , 67.5° , 45° , 22.5° , 11.25° , 165° , 150° , 120° , 105° , 75° , 60° , 30° , 15° and 7.5° .
 3. divide the sum of regular angles with the total number of angles

1.4.7 ANGLE DIVISIBILITY

Let A be the total number of angles in the pattern.

Let A_D be the number of angles divisible by another angle around each vertex.

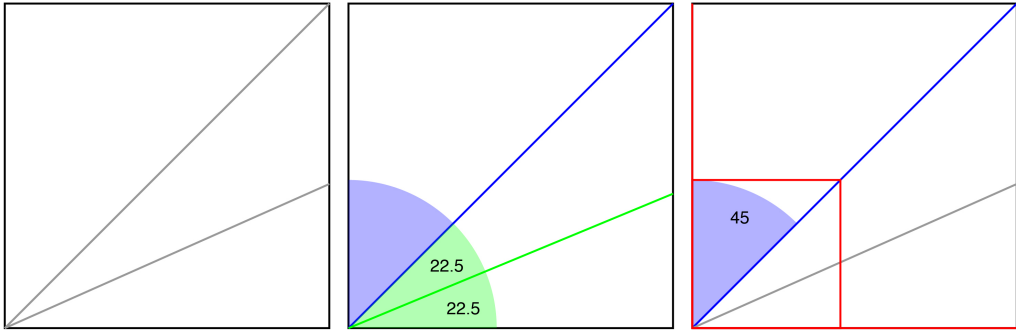


Figure 1.3: Angle Divisibility: from left a sample set of folds around a vertex (bottom left), 90, 45 and 22.5°. The angles of 45 can be halved to give a matching 22.5 or, 22.5° doubled to give a 45° angle. Additionally 45° can be doubled to give 90° shown here as the sheet corner, however this vertex could also be placed in the middle of a sheet.

$$AngleDivisibility = \frac{A_D}{A} \quad (1.7)$$

Angle Divisibility is based on the useful property of Origami Axiom 3 (See Figure 1.2). In this case where the lines intersect this axiom results in *angle bisection*. Using two existing folds we can create and find an additional fold.

An approximation of this property in a crease pattern can be evaluated by comparing every angle in the pattern to a doubled or halved value of all other angles. The complete set of angles is doubled or halved, and intersections calculated between the generated set and the original angle set. A possible advantage to this method is that it may pick instances of this property made by folding more than one layer at a time. However, a more localised method is to iterate over each vertex and evaluate doubled and halved values of every angle in the vertex set.

To measure Angle Divisibility in the set of crease patterns, a script evaluates a flattened mesh of the crease pattern by doing the following:

- Angle Divisibility**
1. calculate the angle of each fold line (edge) around each vertex.
 2. double each angle and halve each angle, and compare to the original angles.
 3. sum each matching divisibility instance.
 4. sum the total of all divisible angles and divide by the total number of angles.



Figure 1.4: **Fold Density** shown in increasing widths of fold from left to right. The net fold density ranges from 0.9, 0.5, 0.1

1.4.8 FOLD DENSITY

Let F_{area} **be** the total area of the creases, calculated as the total length of folds multiplied by the fold width.

Let S_{area} **be** the total area of the sheet.

$$FoldDensity = 1 - \frac{F_{area}}{S_{area}} \quad (1.8)$$

Fold Density is expressed a ratio fold area F_{area} vs sheet area S_{area} , and requires a value for thickness of the material, where $FoldWidth = \pi \times Thickness$. Our measurements are in mm, and default thickness is calculated at 0.1mm for paper media. Fold-area is the total length of folds multiplied by $FoldWidth$, and the area is calculated from the total area of each face. Fold Density reduces when the number of folds increases, or the width of the folds increases. Looking at Figure 1.4 it is clear to see that a Fold Density between 0.0–0.5 is preferred over higher values.

Fold Density 1. sum the lengths of each crease.

2. calculate the area of the pattern
3. divide the sum of fold area by the sheet area and subtract from one.

1.5 Results

The following results are evaluations of experiments conducted during my research.

1.5.1 A NOTE ON FILE NAMING CONVENTIONS

e.g. **orivertex-K10.13-M**

{projectname}-{Pattern Prefix}{U}.{V}-{geometry type}

- **U & V** The grid resolution of the pattern U for horizontal, V for vertical. The higher the values for U & V the more dense the pattern will be.
- **Geometry Types**
 - **Mesh or M:** usually an STL file containing the 3D geometry
 - **Flat Mesh or FM:** usually an STL file containing a flattened crease pattern from the 3D geometry
 - **Render or R:** usually a PNG file containing a lit render of the 3D geometry
- **Fold Unit Prefixes:** A single letter prefix for the pattern, see Table 1.1.

Table 1.1: Fold Unit Prefixes in file naming

Folding pattern	Prefix	Named after
Miura 45	M45.	Koryo Miura
Miura 6090	M60.	Koryo Miura
Yoshimura	Y	Yoshimura
Waterbomb	WB	Traditional Origami
Kresling	K	Biruata Kresling
Resch 3	R3.	Ronald Resch
Resch 4	R4.	Ronald Resch
Resch 6	R6.	Ronald Resch
Huffman Grid ³	H	David Huffman

1.5.2 METRIC ABBREVIATIONS

The metrics are abbreviated in Tables, Graphs and Figures as follows:

- **AD:** Angle Divisibility
- **AE:** Angle Equality
- **AR:** Angle Regularity
- **AU:** Angle Uniqueness
- **FDI:** Fold Density Inverse
- **LE:** Length Equality

³Robert Lang in (Lang, 2017) called this pattern, essentially a Yoshimura pattern, with extended edges that form a hexagonal grid the Huffman Grid, after David Huffman.

- **LEI:** Length Equality Inverse
- **P:** Parallelity

1.5.3 TESTING SQUARE MAPPED FOLD UNITS FOR REGULARITY

The following sets of results are based on comparisons between CAD drafted high-regularity patterns, and patterns generated by planar input to ORI * gh Pattern Generator. The former are the most regular versions of the patterns, as can be seen in the results in Table 1.2 and Figure 1.5. Comparisons between the CAD and ORI * gh are within 0.1 points of R.I.. All the regular versions of the pattern score above 0.9. The R.I. values change dramatically for irregular results, see Table 1.4 and Figure 1.6. Figure 1.6 is the most comprehensive view of the data, as it shows the crease patterns, and the R.I. graphs. This set of patterns was used to calibrate the R.I. metrics during development of the Python script. I found that my first global approximation of Angle Divisibility swayed the results significantly, and so I implemented a per vertex evaluation to localise and increase accuracy of the matches. *Angle Divisibility* criterion is rarer, and so patterns that are otherwise similarly regular only get over 90% regularity with scores in Angle Divisibility. For example, the waterbomb and Resch4 patterns are highly regular, scoring the highest R.I. rank in testing. This is due to 45° crosses and 90° corners, which score highly on both *Angle Regularity* and *Angle Divisibility*.

1.5.3.1 CAD drafted pattern

Figure 1.5 and Table 1.2 show high-regularity natural folding patterns and their associated R.I. graphs. Nearly all of these patterns are readily foldable in paper by hand requiring simple angular and sheet divisions. The exception is M60, where folding the pattern requires overcoming the periodic parallelity of line, and the low availability of adjacent angles suggested by its low score in AD. Generally though, it can be seen that with R.I. values above 0.9, the pattern is likely to be hand foldable. The exception of an individual low scores below 0.5, suggests that the whole index - all values - must be taken into consideration in evaluating the patterns foldability.

Table 1.2: R.I. Square Mapped Results, decreasing regularity **AD**:Angle Divisibility, **AE**:Angle Equality, **AR**:Angle Regularity, **AU**:Angle Uniqueness, **FDI**:Fold Density Inverse, **LE**:Length Equality, **LEI**:Length Equality Inverse, **P**:Parallelity, **R.I.**:Origami Regularity Index

Pattern	AD	AE	AR	AU	FDI	LE	LEI	P	R.I.
WB13.13	0.997	1.0	1.0	0.99	0.94	1.0	0.99	1.0	0.992
R4-10.10	0.996	1.0	1.0	0.99	0.96	1.0	0.99	1.0	0.992
Y11.11	0.97	1.0	1.0	0.99	0.96	1.0	0.98	1.0	0.989
M45.11.11	0.9	1.0	1.0	0.99	0.96	1.0	0.99	1.0	0.981
H12.11	0.9	1.0	1.0	0.99	0.97	1.0	0.97	1.0	0.979
M60.10.10	0.395	1.0	1.0	0.99	0.97	1.0	0.99	1.0	0.919

1.5.3.2 ORI * gh generated patterns

Patterns illustrated in Figure 1.6 and evaluations in Tables 1.3 and 1.4 compare regular patterns generated in ORI * gh, called Square Regular: SR, and Square Irregular: IR patterns generated from a distorted square plane. The evaluation covers five Natural Folding patterns, Yoshimura, Huffman, Miura45, Waterbomb, and Resch4. The pattern of R.I. divergence in the SR patterns is consistent, where AD is consistently low in each pattern. Interestingly, in the Square Irregular patterns, created by placing a symmetrical diagonal line, causing a line from top left to bottom right of corner to corner compression, causes a similar pattern of distortion in the R.I. graphs. Each graph has a similar structure where P, LE, FDI, AE remain high, but AD, AR and LEI drop in values. The radar graph makes this similarity in distortion clear. Column 1 in Figure 1.6 is related to Table 1.3, and Column 2 is related to Table 1.3.

Table 1.3: Regular Outputs from ORI * gh using low resolution mapping and square plane geometry

Pattern	AD	AE	AR	AU	FDI	LE	LEI	P	R.I.
SR-Y.13.13	0.937	1.0	0.846	0.991	0.933	1.0	0.987	1.0	0.962
SR-H.13.13	0.917	1.0	0.833	0.986	0.952	1.0	0.969	1.0	0.957
SR-M45.13.13	0.776	1.0	0.849	0.99	0.932	1.0	0.988	0.997	0.942
SR-WB.13.13	0.926	1.0	0.167	0.984	0.921	1.0	0.97	1.0	0.871
SR-R4.18.18	0.842	1.0	0.419	0.993	0.915	0.99	0.987	0.997	0.894

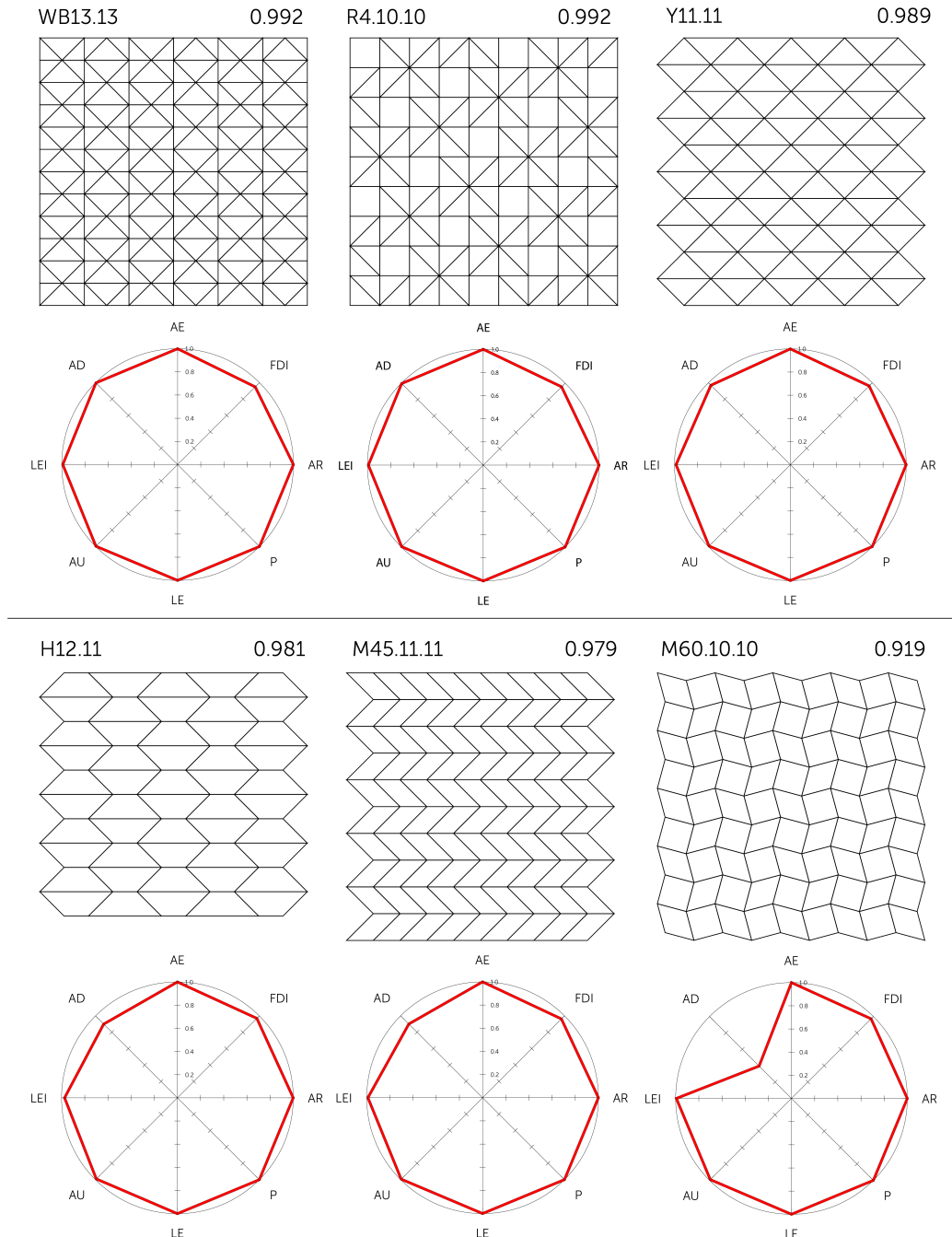


Figure 1.5: Square High-Regularity Crease Patterns and R.I. Graphs. From top left: Waterbomb WB13.13 (0.992), Resch4 R4.10.10 (0.992), Yoshimura Y11.11 (0.989), Miura45 M45.11.11 (0.981), Huffman H12.11 (0.979), Miura60 M60.10.10 (0.919)

Table 1.4: Irregular Outputs from ORI * gh using low resolution mapping and distorted plane geometry

Pattern	AD	AE	AR	AU	FDI	LE	LEI	P	R.I.
IR-Y.13.13	0.0	1.0	0.004	0.588	0.93	1.0	0.735	1.0	0.894
IR-H.13.13	0.0	1.0	0.0	0.763	0.951	1.0	0.634	0.863	0.651
IR-M45.13.13	0.0	0.949	0.006	0.554	0.929	0.98	0.801	0.964	0.647
IR-WB.13.13	0.017	1.0	0.026	0.699	0.918	1.0	0.589	0.806	0.632
IR-R4.18.18	0.015	0.995	0.007	0.59	0.915	0.99	0.64	0.714	0.609

1.5.4 TIMED FOLDING EXPERIMENTS

The timed folding experiments, discussed in the thesis chapter 7, were folded in laser score paper and FPT. The timed measurements were averaged out to folds-per-second as a method to verify increased foldability of FPTs, however a parallel experiment was to validate the effectiveness of the R.I. as a predictor of foldability, where speed of folding could be considered a basic factor in validation. A correlation between folds-per-second and R.I. index could show that the R.I. value as a predictor of difficulty. The results are preliminary, and show some correlation between the R.I. and foldability when measured by speed. The validation shown by this data is insufficient to conclusively show a relationship, but it is some evidence that the subject is worthwhile further research that could lead to a verifiable method for determining irregularity-based foldability.

Table 1.5: R.I. Summary of Timed Folding Experiments discussed in the thesis chapter 7, ranked by R.I.

Pattern	AD	AE	AR	AU	FDI	LE	LEI	P	R.I.
M45.25.25	0.96	1.00	1.00	0.99	0.95	1.00	0.99	1.00	0.988
ORIBOzuru	0.23	0.93	0.14	0.62	0.97	0.96	0.56	0.63	0.637
FFDome	0.02	0.99	0.00	0.83	0.97	1.00	0.82	1.00	0.605
R4-31.26	0.01	0.80	0.01	0.55	0.98	0.65	0.40	0.37	0.471

1.5.5 OTHER EXPERIMENTS

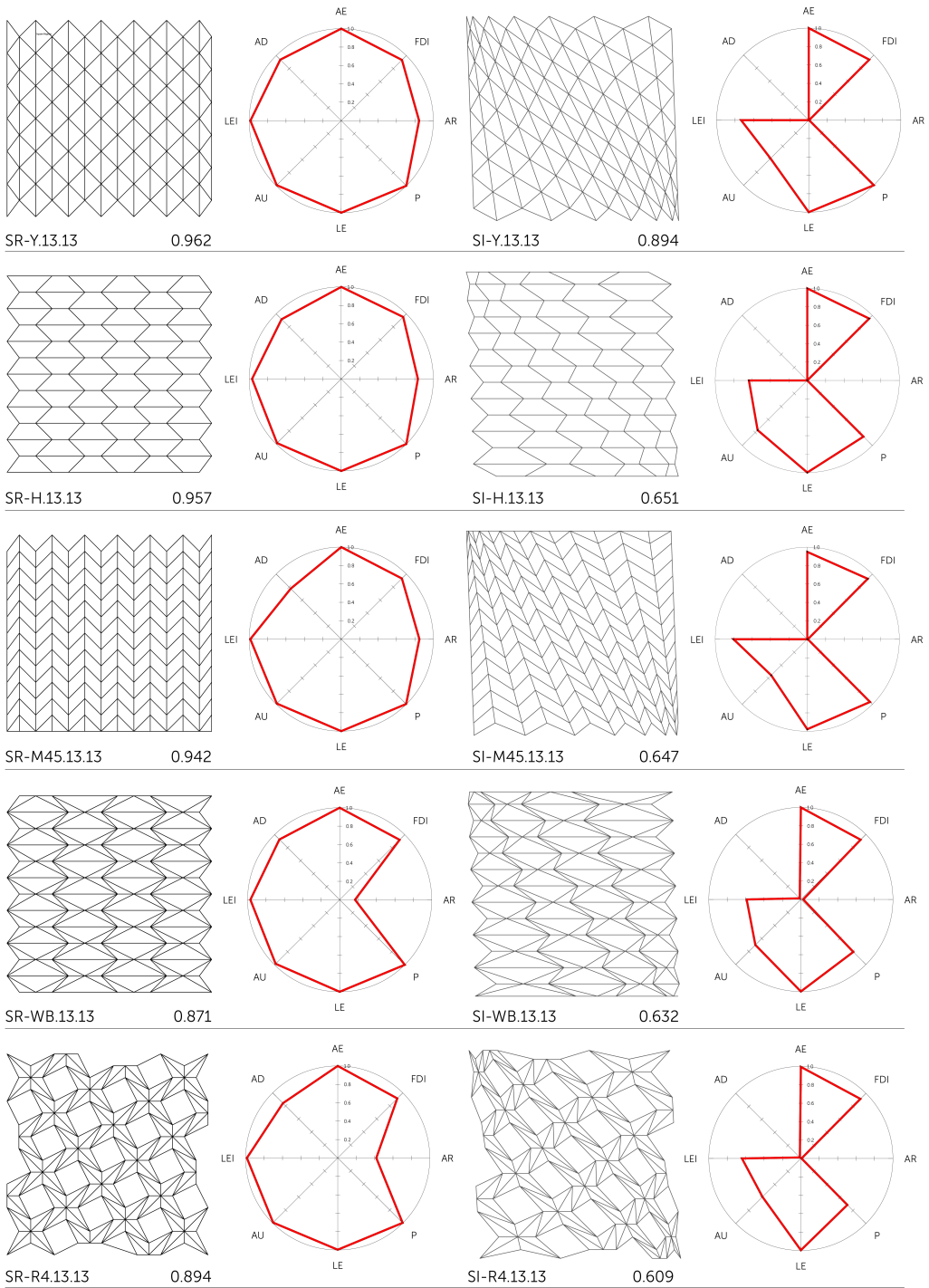


Figure 1.6: Comparison of Square Outputs from $\text{ORI} \star \text{gh}$. Column 1 contains the Square Regular (SR) patterns and graphs, Column 2 contains the Irregular (IR) patterns and graphs.

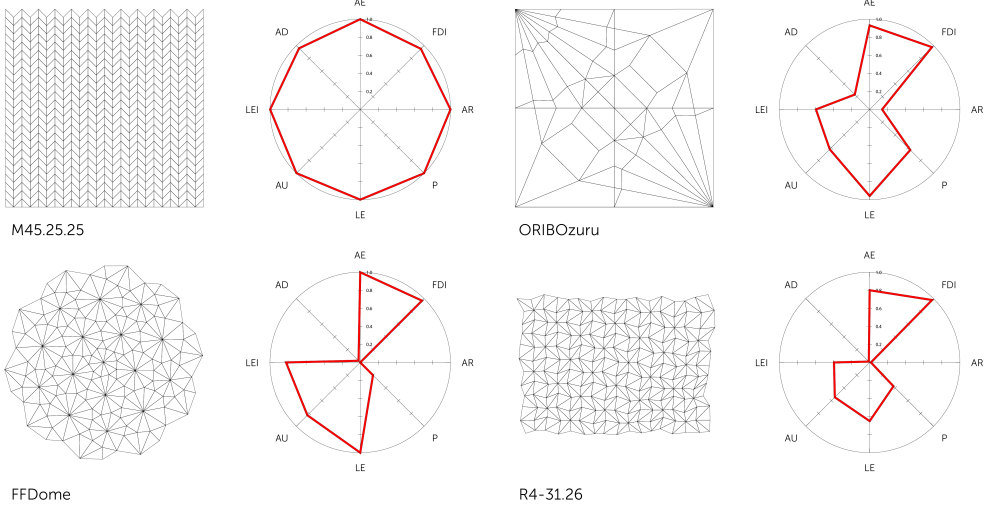


Figure 1.7: Timed Folding Experiments patterns and associated R.I. graphs

Pattern	AD	AE	AR	AU	FDI	LE	LEI	P	R.I.
Breathe-V3.17.18	0.01	0.43	0.01	0.25	0.97	0.31	0.16	0.15	0.286
ORIfox-001	0.00	0.77	0.01	0.54	0.95	0.82	0.55	0.45	0.512

1.5.6 ORI * VERTEX VARIATIONS

Table 1.6: R.I. Summary of Project Based Results, ranked by R.I.

Pattern	AD	AE	AR	AU	FDI	LE	LEI	P	R.I.
orivertex-R4.50.50	0.01	0.97	0.01	0.79	0.93	0.98	0.91	0.78	0.674
orivertex-R4.30.30	0.00	0.76	0.01	0.49	0.95	0.92	0.67	0.42	0.530
orivertex-01WB17.15	0.01	0.73	0.01	0.49	0.95	0.82	0.53	0.35	0.489
orivertextex-K10.13	0.00	0.57	0.01	0.37	0.95	0.45	0.25	0.31	0.368
orivertextex-Y12.9C	0.02	0.41	0.00	0.24	0.98	0.39	0.22	0.14	0.301

1.6 Evaluation

R.I. rankings for various patterns were subjectively validated during the development of the metrics, results showed beginner folds such as the bird-base and regular corrugation rankings were congruent with high R.I. rankings, therefore easy, while difficult patterns with high irregularity scored low, and therefore difficult to fold without digital fabrication. In general, folding patterns less than 0.6 begin to be difficult without digital fabrication methods. The results for verification by time to fold, as discussed in the full thesis document in Chapter 7, are inconsistent for paper according to the division of seconds-per-fold (s/f), with FFDome as the anomaly, the acute folds in ringed clusters of 10 and 12 were difficult to collapse in paper, suggesting that material foldability could be the cause for the anomaly. In FPTECS, when examined as seconds per fold, there is a correlation between

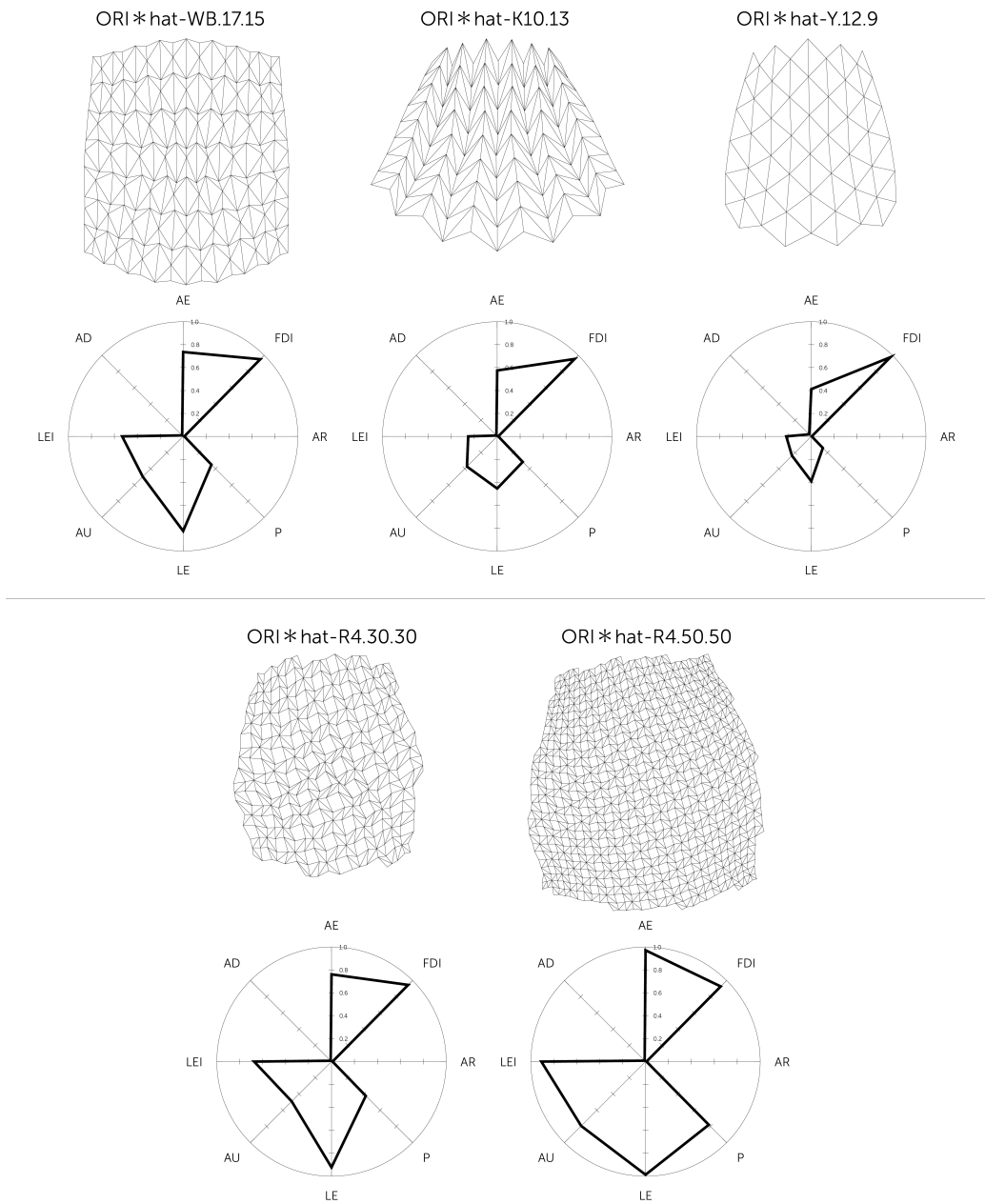


Figure 1.8: ORI * vertex variations shown with their associated R.I. graphs.

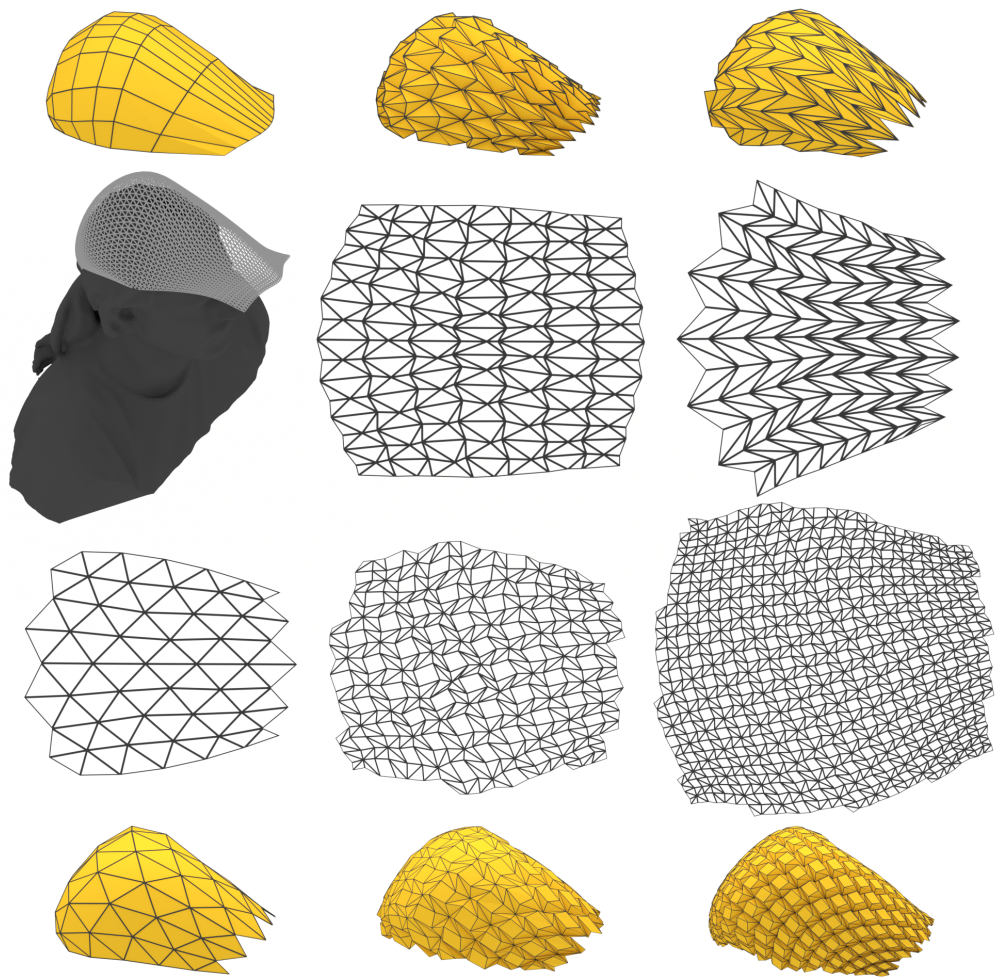


Figure 1.9: ORI \star vertex examples show the variations between each pattern and the sculptural form.

complete evaluation of the Foldability pattern would require some very complex metrics that are currently outside the scope of this research. The R.I. is rather useful in this case, as it averages the geometric properties, giving the researcher an indication of its geometric complexity and thereby foldability.

A limitation to the R.I. implementation is that the metrics are based on non-localised averages, rather than a complex crease-to-crease analysis, which as discussed at the outset was a trade-off between computational complexity involving long analysis times, and adaptability to new metrics. This R.I. implementation shows correlations with folding difficulty, however, it is plausible that the metric set is not yet complete. This could be evaluated with a larger data-set, cross-referenced with subjective difficulty evaluations and fold-times. The simplicity of the R.I. gives generalised, numeric, evaluations of irregularity in a crease pattern, and this can indicate foldability complexity, and its details give clear understanding of what irregularities exist and could therefore indicate how to improve a design for foldability. A Resch4 pattern shown in Chapter 7, for example, with 0.471 R.I. could be almost doubled to 0.87 R.I. by making the pattern perfectly regular, and be folded easily and accurately by-hand, at 0.471 it is very difficult by-hand. Without doubt, irregular patterns are very difficult to fold *by-hand*, and with fabrication technologies, the complexity is significantly reduced. For the purpose of evaluating this small set of patterns, the R.I. met its goal for establishing a numeric index to differentiate regularity from one folding pattern to the next, thus allowing the researcher to judge the clear foldability benefits of a given pattern and to evaluate the most suitable fabrication technique.

1.7 Source

The script is written in Blender Python, and is archived on github, as the source file from [https://github.com/oribotic/Origami-Regularity-Index⁴](https://github.com/oribotic/Origami-Regularity-Index) and a Blender file with sample geometries for testing. Blender can be downloaded from <http://www.blender.org/>

Basic Instructions: Import your crease pattern as a welded mesh with no duplicate vertices, select the object and press “run script” button, and the script will write several text files in the source directory, including a summary file showing a table of detailed R.I. values, and a detail file that contains each individual line and angle used in the calculation.

⁴<https://github.com/oribotic/Origami-Regularity-Index>

Bibliography

- Bern, M., Hayes, B., 1996. The complexity of flat origami, in: SODA. pp. 175–183.
- Demaine, E., Tachi, T., 2010. Origamizer: A practical algorithm for folding any polyhedron. Manuscript.
- Demaine, E.D., Demaine, M.L., 2002. Recent results in computational origami, in: Origami3: Third International Meeting of Origami Science, Mathematics and Education. pp. 3–16.
- Dudte, L.H., Vouga, E., Tachi, T., Mahadevan, L., 2016. Programming curvature using origami tessellations. *Nature materials*.
- Hull, T., 1994. On the mathematics of flat origamis. *Congressus numerantium* 215–224.
- Kasahara, K., Takahama, T., 1998. Origami for the Connoisseur. Japan Pubns.
- Kawasaki, T., 1989. On relation between mountain-creases and valley-creases of a flat origami, in: Huzita, H. (Ed.), *Proceedings of the First International Meeting of Origami Science and Technology*. Ferrara, pp. 229–237.
- Lang, R., 2017. Twists, Tilings, and Tessellations: Mathematical Methods for Geometric Origami. CRC Press.
- Lang, Robert, 2007. ReferenceFinder | Robert J. Lang Origami.
- OrigamiUSA, n.d. Guidelines for Origami Difficulty | OrigamiUSA [WWW Document]. URL <https://origamiusa.org/difficulty> (accessed 6.14.18).
- Paperboard, I., 1993. Paperboard reference manual. Iggesund Paperboard, Sweden.
- Tachi, T., 2010. Freeform origami.
- Tachi, T., 2010. Freeform variations of origami. *J. Geom. Graph* 14, 203–215.
- Tachi, T., 2009. Generalization of rigid foldable quadrilateral mesh origami. Symposium of the International Association for Shell and Spatial Structures p. 2287–2294.
- Tachi, T., 2007. Rigid Origami Simulator. Tokyo, Japan.